

EUV Observation with Normal Incidence Multilayer Telescopes

HIDEYO KUNIEDA,¹ KOUJUN YAMASHITA,¹
TAKASHI YAMAZAKI,¹ KAZUAKI IKEDA,¹
KAZUTAMI MISAKI,¹ YOSHIYUKI TAKIZAWA,²
MASATO NAKAMURA,² ICHIRO YOSHIKAWA,²
AND ASAMI YAMAGUCHI³

¹Department of Physics, Nagoya University, Nagoya 464-01

²Department of Earth and Planetary Physics, University of Tokyo, Tokyo 113

³National Astronomical Observatory, Mitaka 181

The EUV emission from hot interstellar plasmas is observed by normal incidence telescopes on board a sounding rocket. It was performed on January 29, 1995, to observe the sky area around the HZ 43 close to the north galactic pole. The wave bands ($\delta\lambda \sim 10 \text{ \AA}$) are provided at 130 and 170 \AA by the multilayer coating on the reflectors of 20 cm in diameter and of 30 cm in focal length. The focal plane images are detected by CsI coated MCP's. The observed flux of HZ 43 is 1.5 counts s^{-1} at 130 \AA and 3 counts s^{-1} at 170 \AA . The diffuse emission is 27 c/s/deg^2 at 130 \AA and 20 c/s/deg^2 at 170 \AA . Those preliminary numbers are subjects to change along with the data analysis.

1. Introduction

Interstellar field is assumed to be filled with cold gas with dust and thin hot plasmas of about 10^5 to 10^6 K. The latter component has been recognized in soft X-ray observations below 1 keV. The plasmas of 10^6 K is characterized by emission lines from O VII and OVIII at 0.56 and 0.65 keV, respectively, while EUV emission lines are expected from plasmas of lower temperature in 10^5 K range.

Thinner windows were developed to enhance the detection efficiency in longer wavelength range for the proportional counters. However, strong contamination was found due to the He II (304 \AA) emission lines from geocorona. The diffuse EUV emission is difficult to separate from such strong geocorona emission, because spectrometer is not available but filtering, which allows only factor of ten reduction of He II lines even around the absorption edges.

A breakthrough comes from the progress of X-ray optics. Multilayer coatings, thin layer pairs of light and heavy elements, constructed on mirror surfaces efficiently reflect X-rays of selected wavelength. The first mission to measure celestial objects is performed with *ALEXIS* (see the paper in the same issue). In order to improve sensitivity, large normal incidence telescopes are prepared for a Japanese rocket mission in two wave bands at 130 and 170 \AA to observe the sky region around the brightest EUV source HZ 43. The flight was successful and some complex structure of EUV emission is observed together with a bright point source, HZ 43.

2. Emission Lines from Hot Interstellar Medium

Kato (1976) calculated radiation of a hot thin plasmas from 1 to 250 \AA . The lower temperature plasmas than 10^6 K are expected to emit EUV lines. Figure 1 shows the line emission power in various wavelength bands as a function of temperature (quoted

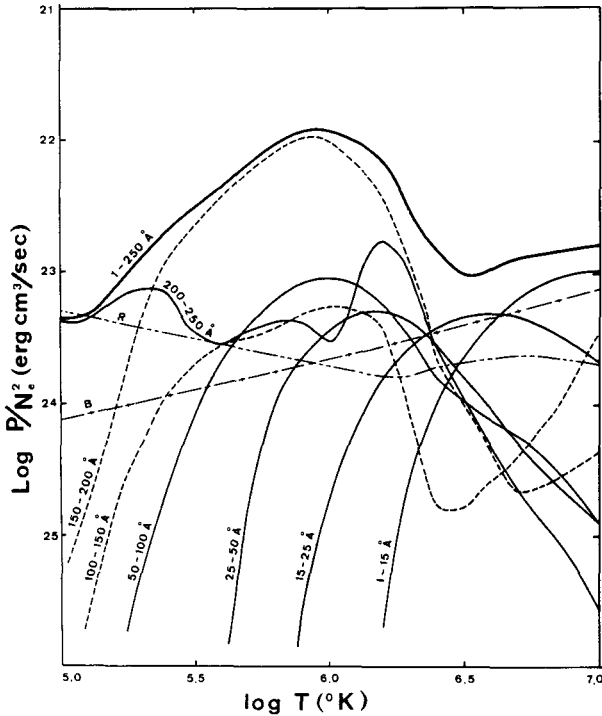


FIGURE 1. Line emission power vs. T .

from Fig. 4 of Kato 1976). The plasmas below 10^6 K are characterized by strong lines in 150–200 Å. Covering 10–100 Å, very soft X-ray detectors only detect the small portion of energy flux from cooler gas. The calculated spectrum of 8×10^5 K is shown in Fig. 2 in wave length range from 100 through 250 Å (Fig. 3 of Kato 1976). The strongest lines are found at around 170 Å, all emerged from ionized iron ions (Fe IX 171.06 Å, Fe X 170.9 Å). Below 140 Å, no lines are seen more than 1/100 of the strongest one at 170 Å.

Our strategy is to provide one pass band at 170 Å to get those strong lines and another band at 130 Å to put a limit of continuum flux without line emission. The lines at 170 Å have strong temperature dependence, which is clear in the Fig. 1.

3. Instrumentation

3.1. Multilayer Normal Incidence Telescopes

Since the two wave bands at 130 and 170 Å are favorable to decide the physical situation of hot plasmas at the temperature of $10^5 - 10^6$ K, 2d of multilayer coatings are tuned to be 140 Å and 184 Å with 20 and 25 layer pairs of Mo/Si, respectively. The reflectivity measured at a synchrotron facility (UVSOR at the Institute for Molecular Science: Okazaki, Japan) are shown in Fig. 3a and 3b. Peak reflectivity is about 50–60% and the width of pass band is about 10 Å in both cases.

Multilayer structure is coated on a spherical mirror of 20 cm in diameter and 30 cm in focal length. Polishing and coatings were done by Nikon. It is placed at the bottom

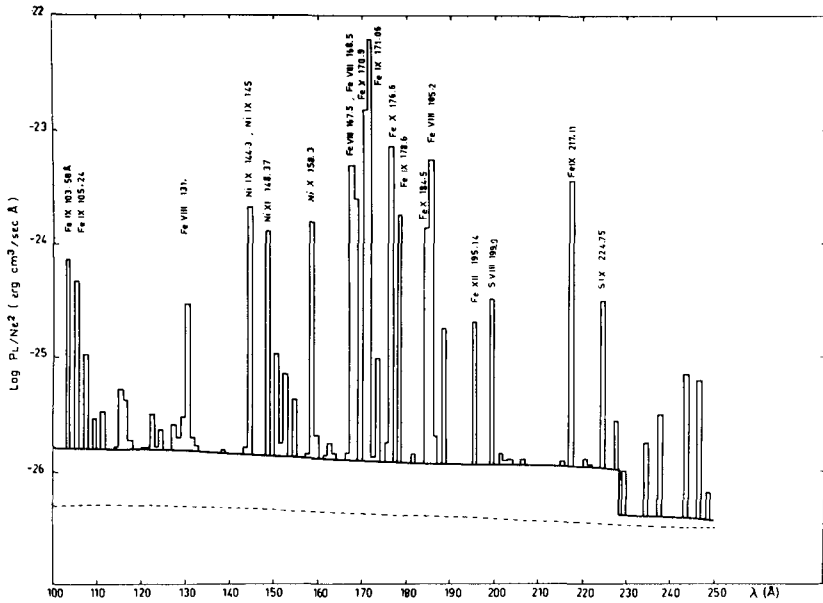


FIGURE 2. Spectrum of plasma of 8×10^5 K.

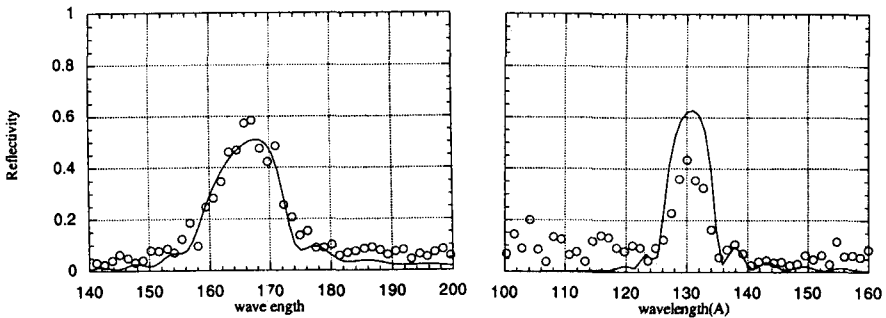


FIGURE 3. (a) Mirror reflectivity (NIT-1). (b) Mirror reflectivity (NIT-2).

of a housing, whose cross section is shown in Fig. 4. A micro-channel plate of 28 mm in diameter (corresponding field of view of 4 degree) is put on the focal plane. Images are obtained by a regisive plate after the two stage MCP. The CsI coating on the MCP yields detection efficiency of about 20% at 130–170 Å. In order to reject longer wave light C filter of 1200 Å is placed in front of MCP. The inflow of the ambient plasmas is rejected by a mesh at the entrance window. The normal incidence telescope for 170 Å is named NIT-1 and that for 130 Å is named NIT-2.

3.2. Helium Line Monitor and UV Star Sensor

Another multilayer telescope (HEM) is equipped to monitor He II lines (304 Å) from geocorona. One more telescope (UVT) with mono-layer coating is prepared as a attitude

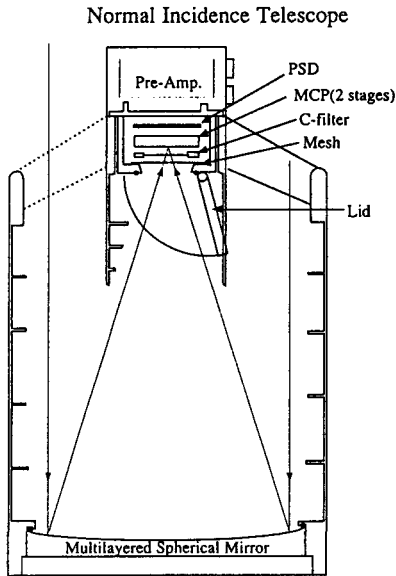


FIGURE 4. Cross section of NIT.

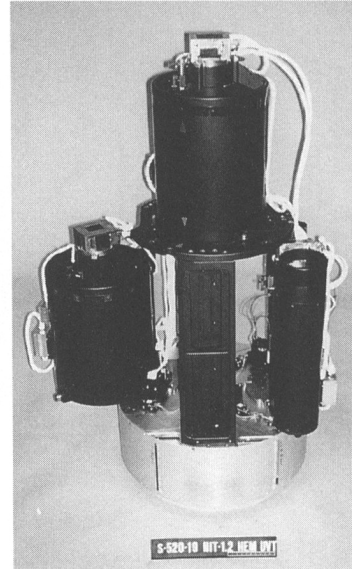


FIGURE 5. Picture of Hole Payload.

sensor with stars in UV band (1600–2800 Å). Four photomultipliers are placed on the focal plane with rotating slits of three different patterns.

NIT-1 is placed at the top of the structure, while NIT-2, UVT and HEM are flooded inside the structure, which are to be deployed after the nose fairing is removed in the sky (Fig. 5). All these instruments are looking at the top direction of the structure.

4. Flight Operation

The telescopes were launched by a rocket S-520-19 at 16:00 (UT) on 1995 January 28 from Kagoshima Space Center of the Institute of Space and Astronautical Science. 40 s after the launch, nose fairing was blown off and the attitude control system, deploy of instruments, and high voltage operations were taken place in sequence. At X + 100 sec in the altitude of more than 150 km, all instruments were ready to observe the sky area around HZ 43. During 300 s pointing observation, payload achieved at the apogee of 350 km. Then the system was rotated 360 degree around the pointing direction for 50 sec. Telemetry data was successfully obtained by the end of our observation, with some short interruptions.

5. Results

5.1. Light Curve

Total counting rate of whole detector is examined for each detector after the start of operation at 100 s. It is almost constant at the level of 300 counts s^{-1} and 500 counts s^{-1} for NIT-1 and NIT-2, respectively, except for the three occasions at 130 s, 180 sec, and 400 s, when the telemetry was lost. Those counting rates could have altitude dependence, if there were some geophysical contaminations due to the air glow and the

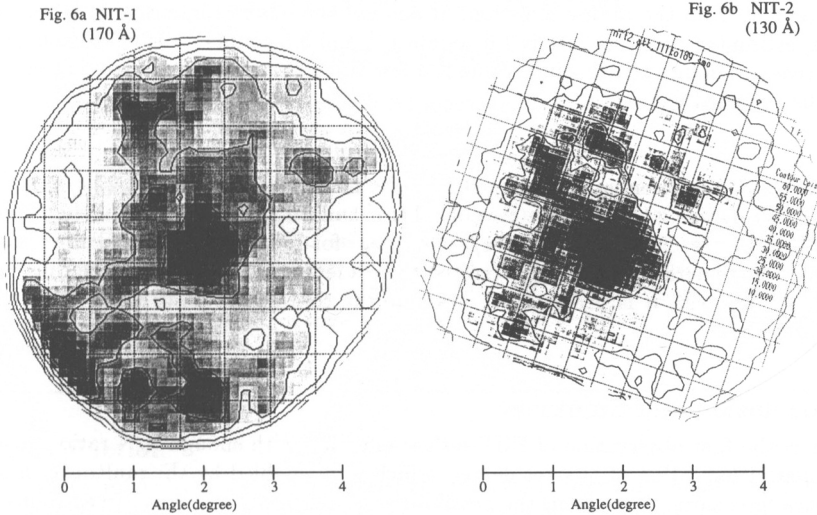


FIGURE 6. (a) NIT-1, 170 Å.

(b) NIT-2, 130 Å.

radiation belts. Electrons trapped by geomagnetic field should be sensitive to the angle between the line of sight and the magnetic field. We are able to put an upper limit of about 10% for the contamination from geophysical origins.

5.2. Images

Fig. 6a shows the NIT-1 image of 170 Å band integrated from X + 200 through X+ 350 s without attitude correction. The bright source at the center is the image of HZ 43. The image size of a point source is estimated to be 0.3 degree or so in this case. Other structure found right top, right bottom and a sort of “peninsula” to the left could be real feature.

Fig. 6b is the NIT-2 image of 130 Å band in the same period of time. The bright source is not so much out standing as in Fig. 6a, but there. Other structures seen in 170 Å image are also found.

6. Discussion

6.1. Detection Efficiency

The effective area and detection efficiency are roughly estimated as follows.

Eff. Area	Ref.	$d\lambda$	Detector	Filter	Mesh	
$(300 \text{ cm}^2) \times$	$(50\%) \times$	$(5 \text{ Å}) \times$	$(20\%) \times$	$(30\%) \times$	(90%)	$= 41 \text{ cm}^2 \text{ Å} (130 \text{ Å})$
$(300 \text{ cm}^2) \times$	$(50\%) \times$	$(10 \text{ Å}) \times$	$(20\%) \times$	$(20\%) \times$	(90%)	$= 54 \text{ cm}^2 \text{ Å} (170 \text{ Å})$

6.2. Intensity of HZ 43

The flux of HZ 43 in both bands is estimated to be 3 and 1.5 counts s^{-1} from the central enhancement from the diffuse emission. If one use the observe intensity of HZ 43 with EUVE, estimated counting rate is 7.6 counts s^{-1} and 3.5 counts s^{-1} for 170 and 130 Å, respectively. Though the absolute value is a few times lower, the flux ratio is consistent with the reported value.

6.3. Diffuse EUV Emission

The observed diffuse emission averaged over the field of view is 20 and 27 $c/s/deg^2$ for 170 and 130 Å. Using the effective area of 5.4 cm^2 and 8.2 cm^2 for a line, the flux of Fe IX at 170 Å is 3.7 $c/s/cm^2/deg^2$ and 3.3 $c/s/cm^2/deg^2$ for 130 Å. If the normal abundance is assumed, the temperature of gas is suggested to be a few time 10^5 based on the calculation in Fig. 1. However, it is necessary to evaluate the contamination to those wave bands very carefully.

7. Conclusion and Summary

This is the first observation of EUV diffuse emission with enough S/N ratio and with good spatial resolution of quarter degree, which were enabled by the multilayer normal incidence telescopes. It confirms the possibilities of multilayer telescopes in astrophysical observations. The data analysis is still going on and the results presented here are subjects to change.

REFERENCES

- KATO, T. 1976, Radiation from Hot Thin Plasmas from 1 to 250 Å, *ApJS*, 30, 397